

# DFT Studies of Alkene Insertions into Cu–B Bonds in Copper(I) Boryl Complexes

Li Dang, Haitao Zhao, and Zhenyang Lin\*

Department of Chemistry, The Hong Kong University of Science and Technology, Clear Water Bay, Kowloon, Hong Kong, People's Republic of China

Todd B. Marder\*

Department of Chemistry, Durham University, South Road, Durham DH1 3LE, U.K.

Received February 2, 2007

DFT calculations have been carried out to study the insertion reactions of alkenes into the Cu–B bond in (NHC)Cu(boryl) complexes (NHC = N-heterocyclic carbene). The nature of the insertion reactions and the relevant regiochemistry have been examined along with  $\beta$ -hydride eliminations, which are followed by reinsertion of the alkene into the Cu–H bond. Hyperconjugation (i.e.,  $\pi$  bonding) between the Cu–C  $\sigma$  bond and the “empty”  $p_z$  orbital on boron has been identified as the cause of the unexpectedly small Cu–C–B angle found experimentally by X-ray diffraction in  $\alpha$ -borylalkyl Cu(I) complexes.

## Introduction

Transition metal boryl complexes<sup>1</sup> play important roles in catalyzed hydroboration, diboration, dehydrogenative borylation, and other B–X addition reactions to unsaturated organics<sup>2–4</sup> as well as the catalyzed borylation of C–H bonds in alkanes and arenes.<sup>5,6</sup> Insertion of alkenes into M–B bonds in boryl complexes<sup>7</sup> has been well established and is critical to a variety

of processes such as alkene diboration<sup>8</sup> and other B–X additions such as silylboration and stannylation reactions<sup>9</sup> as well as the dehydrogenative borylation<sup>10</sup> of alkenes to vinylboronate esters, a process that involves alkene insertion into M–B followed by  $\beta$ -hydride elimination.<sup>9f</sup>

Very recently, Sadighi and co-workers investigated the insertion of styrenes into the Cu–B bond in an N-heterocyclic carbene-ligated copper boryl complex, **1**.<sup>7d</sup> The styrene insertion product, **2**, a  $\beta$ -borylalkyl complex, was isolated and structurally characterized by single-crystal X-ray diffraction. Experimentally, it was also found that, on heating, **2** undergoes a  $\beta$ -hydride elimination/reinsertion sequence to afford a rearranged  $\alpha$ -borylalkyl complex, **3** (Scheme 1). The crystal structure of **3** showed a small Cu–C–B angle of 96.3(2)°. Such a small angle around a formally sp<sup>3</sup>-hybridized carbon is quite unexpected.

\* Corresponding authors. E-mail: chzlin@ust.hk; todd.marder@durham.ac.uk.

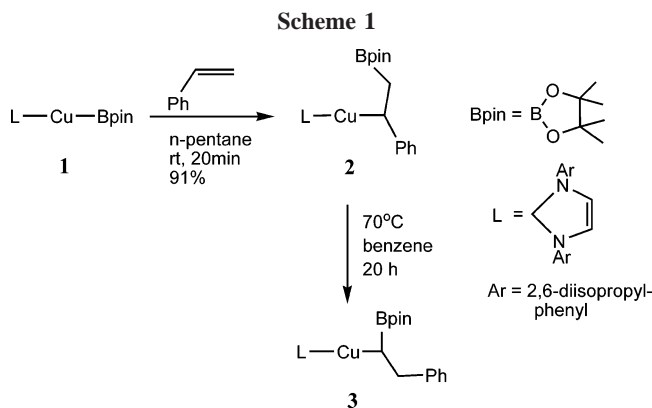
(1) For reviews see: (a) Hartwig, J. F.; Waltz, K. M.; Muhoro, C. N.; He, X.; Eisenstein, O.; Bosque, R.; Maseras, F. In *Advances of Boron Chemistry*; Siebert, W., Ed.; Spec. Publ. No. 201, The Royal Society of Chemistry: Cambridge, 1997; p 373. (b) Wadepohl, H. *Angew. Chem., Int. Ed.* **1997**, *36*, 2441. (c) Irvine, G. J.; Lesley, M. J. G.; Marder, T. B.; Norman, N. C.; Rice, C. R.; Robins, E. G.; Roper, W. R.; Whittell, G. R.; Wright, L. *J. Chem. Rev.* **1998**, *98*, 2685. (d) Braunschweig, H. *Angew. Chem., Int. Ed.* **1998**, *37*, 1786. (e) Smith, M. R., III. *Prog. Inorg. Chem.* **1999**, *48*, 505. (f) Braunschweig, H.; Colling, M. *Coord. Chem. Rev.* **2001**, *223*, 1. (g) Aldridge, S.; Coombs, D. L. *Coord. Chem. Rev.* **2004**, *248*, 535. (h) Braunschweig, H.; Kollann, C.; Rais, D. *Angew. Chem., Int. Ed.* **2006**, *45*, 5254. (i) For a recent structural and computational study, see: Lam, W. H.; Shimada, S.; Batsanov, A. S.; Lin, Z. Y.; Marder, T. B.; Cowan, J. A.; Howard, J. A. K.; Mason, S. A.; McIntyre, G. J. *Organometallics* **2003**, *22*, 4557. (j) Cook, K. S.; Incarvito, C. D.; Webster, C. E.; Fan, Y.; Hall, M. B.; Hartwig, J. F. *Angew. Chem., Int. Ed.* **2004**, *43*, 5474. (k) Lachaize, S.; Essalah, W.; Montiel-Palma, V.; Vendier, L.; Chaudret, B.; Barthelat, J. C.; Sabo-Etienne, S. *Organometallics* **2005**, *24*, 2935.

(2) (a) Manning, D.; Nöth, H. *Angew. Chem., Int. Ed. Engl.* **1985**, *24*, 878. For reviews see: (b) Burgess, K.; Ohlmeyer, M. J. *Chem. Rev.* **1991**, *91*, 1179. (c) Burgess, K.; van der Donk, W. A. In *Encyclopedia of Inorganic Chemistry*; King, R. B., Ed.; Wiley: Chichester, 1994; Vol. 3, p 1420. (d) Fu, G. C.; Evans, D. A.; Muci, A. R. In *Advances in Catalytic Processes*; Doyle, M. P., Ed.; JAI: Greenwich, CT, 1995; p 95. (e) Beletskaya, I.; Pelter, A. *Tetrahedron* **1997**, *53*, 4957. (f) Crudden, C. M.; Edwards, D. *Eur. J. Org. Chem.* **2003**, 4695.

(3) For reviews, see: (a) Marder, T. B.; Norman, N. C. *Top. Catal.* **1998**, *5*, 63. (b) Ishiyama, T.; Miyaura, N. *J. Synth. Org. Chem. Jpn.* **1999**, *57*, 503. (c) Ishiyama, T.; Miyaura, N. *J. Organomet. Chem.* **2000**, *611*, 392. (d) Ishiyama, T.; Miyaura, N. *Chem. Rec.* **2004**, *3*, 271.

(4) (a) Musaev, D. G.; Mebel, A. M.; Morokuma, K. *J. Am. Chem. Soc.* **1994**, *116*, 10693. (b) Dorigo, A. E.; Schleyer, P. von R. *Angew. Chem., Int. Ed.* **1995**, *34*, 115. (c) Widauer, C.; Grützmacher, H.; Ziegler, T. *Organometallics* **2000**, *19*, 2097. (d) For a review, see: Huang, X.; Lin, Z. In *Computational Modeling of Homogeneous Catalysis*; Maseras, F., Lledós, A., Eds.; Kluwer Academic Publishers: Amsterdam, 2002; pp 189–212. (e) Dembitsky, V. M.; Abu Ali, H.; Srebnik, M. *Appl. Organomet. Chem.* **2003**, *17*, 327.

(5) (a) Iverson, C. N.; Smith, M. R., III. *J. Am. Chem. Soc.* **1999**, *121*, 7696. (b) Waltz, K. M.; Hartwig, J. F. *J. Am. Chem. Soc.* **2000**, *122*, 11358. (c) Chen, H.; Schlecht, S.; Semple, T. C.; Hartwig, J. F. *Science* **2000**, *287*, 1995. (d) Cho, J.-Y.; Iverson, C. N.; Smith, M. R., III. *J. Am. Chem. Soc.* **2000**, *122*, 12868. (e) Tse, M. K.; Cho, J.-Y.; Smith, M. R., III. *Org. Lett.* **2001**, *3*, 2831. (f) Ishiyama, T.; Ishida, K.; Takagi, J.; Miyaura, N. *Chem. Lett.* **2001**, 1082. (g) Shimada, S.; Batsanov, A. S.; Howard, J. A. K.; Marder, T. B. *Angew. Chem., Int. Ed.* **2001**, *40*, 2168. (h) Cho, J.-Y.; Tse, M. K.; Holmes, D.; Maleczka, R. E., Jr.; Smith, M. R., III. *Science* **2002**, *295*, 305. (i) Ishiyama, T.; Tagaki, J.; Ishida, K.; Miyaura, N.; Anastasi, N. R.; Hartwig, J. F. *J. Am. Chem. Soc.* **2002**, *124*, 390. (j) Kondo, Y.; Garcia-Cuadrado, D.; Hartwig, J. F.; Boelen, N. K.; Wagner, N. L.; Hillmyer, M. A. *J. Am. Chem. Soc.* **2002**, *124*, 1164. (k) Takagi, J.; Sato, K.; Hartwig, J. F.; Ishiyama, T.; Miyaura, N. *Tetrahedron Lett.* **2002**, *43*, 5649. (l) Ishiyama, T.; Takagi, J.; Hartwig, J. F.; Miyaura, N. *Angew. Chem., Int. Ed.* **2002**, *41*, 3056. (m) Wan, X.; Wang, X.; Luo, Y.; Takami, S.; Kubo, M.; Miyamoto, A. *Organometallics* **2002**, *21*, 3703. (n) Webster, C. E.; Fan, Y.; Hall, M. B.; Kunz, D.; Hartwig, J. F. *J. Am. Chem. Soc.* **2003**, *125*, 858. (o) Lam, W. H.; Lin, Z. Y. *Organometallics* **2003**, *22*, 473. (p) Tamura, H.; Yamazaki, H.; Sato, H.; Sakaki, S. *J. Am. Chem. Soc.* **2003**, *125*, 16114. (q) Ishiyama, T.; Miyaura, N. *J. Organomet. Chem.* **2003**, *680*, 3. (r) Kurotobi, K.; Miyauchi, M.; Takakura, K.; Murafuji, T.; Sugihara, Y. *Eur. J. Org. Chem.* **2003**, 3663. (s) Ishiyama, T.; Nobuta, Y.; Hartwig, J. F.; Miyaura, N. *Chem. Commun.* **2003**, 2924. (t) Ishiyama, T.; Takagi, J.; Yonekawa, Y.; Hartwig, J. F.; Miyaura, N. *Adv. Synth. Catal.* **2003**, *345*, 1003. (u) Datta, A.; Köllhofer, A.; Plenio, H. *Chem. Commun.* **2004**, 1508. (v) Maleczka, R. E.; Shi, F.; Holmes, D.; Smith, M. R. *J. Am. Chem. Soc.* **2003**, *125*, 7792. (w) Lam, W. H.; Lam, K. C.; Lin, Z.; Shimada, S.; Perutz, R. N.; Marder, T. B. *Dalton Trans.* **2004**, 1556. (x) Martins, K.; Zapf, A.; Beller, M. *J. Mol. Catal.* **2004**, *207*, 21.



In this paper, we report the results of DFT calculations providing the energetics related to the **1**  $\rightarrow$  **2** insertion reaction and the **2**  $\rightarrow$  **3** rearrangement process shown in Scheme 1. This study provides further insight into the nature of alkene insertions into a Cu–B bond and allows us to understand the relative ease of the insertion reaction versus the rearrangement process. We then discuss the factors leading to the small Cu–C–B angle observed in the  $\alpha$ -borylalkyl complex, **3**.

### Computational Details

Molecular geometries of the model complexes were optimized without constraints via DFT calculations using the Becke 3LYP

(6) (a) Coventry, D. N.; Batsanov, A. S.; Goeta, A. E.; Howard, J. A. K.; Marder, T. B.; Perutz, R. N. *Chem. Commun.* **2005**, 2172. (b) Chotana, G. A.; Rak, M. A.; Smith, M. R. *J. Am. Chem. Soc.* **2005**, *127*, 10539. (c) Boller, T. M.; Murphy, J. M.; Hapke, M.; Ishiyama, T.; Miyaura, N.; Hartwig, J. F. *J. Am. Chem. Soc.* **2005**, *127*, 14263. (d) Bae, C. S.; Hartwig, J. F.; Chung, H. Y.; Harris, N. K.; Switek, K. A.; Hillmyer, M. A. *Angew. Chem., Int. Ed.* **2005**, *44*, 6410. (e) Hartwig, J. F.; Cook, K. S.; Hapke, M.; Incarvito, C. D.; Fan, Y. B.; Webster, C. E.; Hall, M. B. *J. Am. Chem. Soc.* **2005**, *127*, 2538. (f) Bae, C.; Hartwig, J. F.; Harris, N. K. B.; Long, R. O.; Anderson, K. S.; Hillmyer, M. A. *J. Am. Chem. Soc.* **2005**, *127*, 767. (g) Ishiyama, T. *J. Synth. Org. Chem. Jpn.* **2005**, *63*, 440. (h) Holmes, D.; Chotana, G. A.; Maleczka, R. E.; Smith, M. R. *Org. Lett.* **2006**, *8*, 1407. (i) Shi, F.; Smith, M. R.; Maleczka, R. E. *Org. Lett.* **2006**, *8*, 1411. (j) Murphy, J. C.; Lawrence, J. D.; Kawamura, K.; Incarvito, C.; Hartwig, J. F. *J. Am. Chem. Soc.* **2006**, *128*, 13684. (k) Paul, S.; Chotana, G. A.; Holmes, D.; Reichle, R. C.; Maleczka, R. E.; Smith, M. R. *J. Am. Chem. Soc.* **2006**, *128*, 15552. (l) Mkhaliid, I. A. I.; Coventry, D. N.; Albesa-Jové, D.; Batsanov, A. S.; Howard, J. A. K.; Perutz, R. N.; Marder, T. B. *Angew. Chem., Int. Ed.* **2006**, *45*, 489. (m) Murphy, J. M.; Tzschucke, C. C.; Hartwig, J. F. *Org. Lett.* **2007**, *9*, 757. (n) Tzschucke, C. C.; Murphy, J. M.; Hartwig, J. F. *Org. Lett.* **2007**, *9*, 761. (o) Lo, W. F.; Kaiser, H. M.; Spannenberg, A.; Beller, M.; Tse, M. K. *Tetrahedron Lett.* **2007**, *48*, 371.

(7) (a) Baker, R. T.; Calabrese, J. C.; Westcott, S. A.; Nguyen, P.; Marder, T. B. *J. Am. Chem. Soc.* **1993**, *115*, 4367. (b) Burgess, K.; van der Donk, W. A.; Westcott, S. A.; Marder, T. B.; Baker, R. T.; Calabrese, J. C. *J. Am. Chem. Soc.* **1992**, *114*, 9350. (c) Westcott, S. A.; Blom, H. P.; Marder, T. B.; Baker, R. T. *J. Am. Chem. Soc.* **1992**, *114*, 8863. (d) Laitar, D. S.; Sadighi, J. P. *Organometallics* **2006**, *25*, 2405.

(8) (a) Baker, R. T.; Nguyen, P.; Marder, T. B.; Westcott, S. A. *Angew. Chem., Int. Ed. Engl.* **1995**, *34*, 1336. (b) Ishiyama, T.; Yamamoto, M.; Miyaura, N. *Chem. Commun.* **1997**, 689. (c) Iverson, C. N.; Smith, M. R., III. *Organometallics* **1997**, *16*, 2757. (d) Cui, Q.; Musaev, D. G.; Morokuma, K. *Organometallics* **1997**, *16*, 1355. (e) Marder, T. B.; Norman, N. C.; Rice, C. R. *Tetrahedron Lett.* **1998**, *39*, 155. (f) Dai, C. Y.; Robins, E. G.; Scott, A. J.; Clegg, W.; Yufit, D. S.; Howard, J. A. K.; Marder, T. B. *J. Chem. Soc., Chem. Commun.* **1998**, 1983. (g) Nguyen, P.; Coapes, R. B.; Burke, J. M.; Howard, J. A. K.; Marder, T. B. *J. Organometal. Chem.* **2002**, *652*, 77. (h) Morgan, J. B.; Miller, S. P.; Morken, J. P. *J. Am. Chem. Soc.* **2003**, *125*, 8702. (i) Miller, S. P.; Morgan, J. B.; Nepveux, F. J.; Morken, J. P. *Org. Lett.* **2004**, *6*, 131. (j) Kalendra, D. M.; Dueñas, R. A.; Morken, J. P. *Synlett* **2005**, 1749. (k) Trudeau S.; Morgan, J. B.; Shrestha, M.; Morken, J. P. *J. Org. Chem.* **2005**, *70*, 9538. (l) Ramírez, J.; Corberán, R.; Sanaú, M.; Peris, E.; Fernandez, E. *Chem. Commun.* **2005**, 3056. (m) Ramírez, J.; Segarra, A. M.; Fernandez, E. *Tetrahedron: Asymmetry* **2005**, *16*, 1289. (n) Corberam, R.; Ramírez, J.; Poyatos, M.; Peris, E.; Fernández, E. *Tetrahedron: Asymmetry* **2006**, *17*, 1759. (o) Lillo, V.; Mata, J.; Ramírez, J.; Peris, E.; Fernández, E. *Organometallics* **2006**, *25*, 5829. (p) Lillo, V.; Fructos, M. R.; Ramírez, J.; Braga, A. A. C.; Maseras, F.; Mar Díaz-Requejo, M.; Pérez, P. J.; Fernández, E. *Chem.–Eur. J.*, in press.

(B3LYP)<sup>11</sup> functional. Frequency calculations at the same level of theory have also been performed to identify all the stationary points as minima (zero imaginary frequencies) or transition states (one imaginary frequency) and to provide free energies at 298.15 K, which include entropic contributions by taking into account the vibrational, rotational, and translational motions of the species under consideration. Transition states were located using the Berny algorithm. Intrinsic reaction coordinates (IRC)<sup>12</sup> were calculated for the transition states to confirm that such structures indeed connect two relevant minima. The 6-311G\*\* Pople basis set<sup>13</sup> was used for B, alkenic C atoms in the alkene substrates, and H involved in  $\beta$ -elimination, while the 6-311G\* Wachters–Hay basis set<sup>14</sup> was used for Cu. For all other atoms, the 6-31G basis set was used.<sup>15</sup> To examine the basis set dependence, we also employed a larger basis set to do single-point energy calculations for several selected structures. In the large basis set, 6-311G\*\* was used for B, alkenic C atoms in the alkene substrates, and H involved in  $\beta$ -elimination, while the 6-311G\* Wachters–Hay basis set was used for Cu and 6-31G\* basis set for all other atoms. The results show that the basis set dependence is insignificant. For example, using the smaller basis set, the relative energies of **1N1**, **TS1**, **2A**, and **3A** (Figure 1a) are  $-13.0$ ,  $0.4$ ,  $-26.5$ , and  $-31.1$  kcal/mol, respectively. Using the larger basis set, the relative energies are  $-14.1$ ,  $-1.0$ ,  $-29.4$ , and  $-34.1$  kcal/mol, respectively. We did not test the functional dependence, as the functional used in the calculations reproduces very well the X-ray crystal structures of complexes **2** and **3** (see discussion in the main text). Molecular orbitals obtained from the B3LYP calculations were plotted using the Molden 3.7 program written by Schaftenaar.<sup>16</sup> All of the DFT calculations were performed with the Gaussian 03 package.<sup>17</sup>

### Results and Discussion

**Energetics of the Insertion (1  $\rightarrow$  2) and Rearrangement (2  $\rightarrow$  3) Processes.** As mentioned in the Introduction, the

(9) (a) Suginome, M.; Ito, Y. *Chem. Rev.* **2000**, *100*, 3221. (b) Han, L.-B.; Tanaka, M. *Chem. Commun.* **1999**, 395. (c) Miyaura, N. In *Catalytic Heterofunctionalization*; Togni, A., Grützmacher, H., Eds.; Wiley-VCH: Chichester, 2001; Chapter 1. (d) Onozawa, S.; Tanaka, M. *J. Synth. Org. Chem. Jpn.* **2002**, *60*, 826. (e) Beletskaya, I.; Moberg, C. *Chem. Rev.* **2006**, *106*, 2320. (f) For a recent example of  $\beta$ -hydride elimination during attempted Si–B addition to 1,3-dienes, see: Gerdin, M.; Moberg, C. *Org. Lett.* **2006**, *8*, 2929.

(10) (a) Brown, J. M.; Lloyd-Jones, G. C. *J. Chem. Soc., Chem. Commun.* **1992**, 710. (b) Westcott, S. A.; Marder, T. B.; Baker, R. T. *Organometallics* **1993**, *12*, 975. (c) Brown, J. M.; Lloyd-Jones, G. C. *J. Am. Chem. Soc.* **1994**, *116*, 866. (d) Motry, D. H.; Smith, M. R., III. *J. Am. Chem. Soc.* **1995**, *117*, 6615. (e) Baker, R. T.; Calabrese, J. C.; Westcott, S. A.; Marder, T. B. *J. Am. Chem. Soc.* **1995**, *117*, 8777. (f) Motry, D. H.; Brazil, A. G.; Smith, M. R., III. *J. Am. Chem. Soc.* **1997**, *119*, 2743. (g) Murata, M.; Watanabe, S.; Masuda, Y. *Tetrahedron Lett.* **1999**, *40*, 2585. (h) Vogels, C. M.; Hayes, P. G.; Shaver, M. P.; Westcott, S. A. *Chem. Commun.* **2000**, 51. (i) Kadlecck, D. E.; Carroll, P. J.; Sneddon, L. G. *J. Am. Chem. Soc.* **2000**, *122*, 10868. (j) Murata, M.; Kawakita, K.; Asana, T.; Watanabe, S.; Masuda, Y. *Bull. Chem. Soc. Jpn.* **2002**, *75*, 825. (k) Waltz, K. M.; Muhoro, C. N.; Hartwig, J. F. *Organometallics* **1999**, *18*, 3383. (l) Coapes, R. B.; Souza, F. E. S.; Thomas, R. L.; Hall, J. J.; Marder, T. B. *Chem. Commun.* **2003**, 614.

(11) (a) Becke, A. D. *J. Chem. Phys.* **1993**, *98*, 5648. (b) Miehlich, B.; Savin, A.; Stoll, H.; Preuss, H. *Chem. Phys. Lett.* **1989**, *157*, 200. (c) Lee, C.; Yang, W.; Parr, G. *Phys. Rev. B* **1988**, *37*, 785. (d) Stephens, P. J.; Devlin, F. J.; Chabalowski, C. F. *J. Phys. Chem.* **1994**, *98*, 11623.

(12) (a) Fukui, K. *J. Phys. Chem.* **1970**, *74*, 4161. (b) Fukui, K. *Acc. Chem. Res.* **1981**, *14*, 363.

(13) Krishnan, R.; Binkley, J. S.; Seeger, R.; Pople, J. A. *J. Chem. Phys.* **1980**, *72*, 650.

(14) Hay, P. J.; Wadt, W. R. *J. Chem. Phys.* **1985**, *82*, 299.

(15) Gordon, M. S. *Chem. Phys. Lett.* **1980**, *76*, 163. (b) Hariharan, P. C.; Pople, J. A. *Theor. Chim. Acta* **1973**, *28*, 213. (c) Binning, R. C., Jr.; Curtiss, L. A. *J. Comput. Chem.* **1990**, *11*, 1206.

(16) Schaftenaar, G. *Molden v3.7*; CAOS/CAMM Center Nijmegen: Toernooiveld, Nijmegen, Netherlands, 2001.

(17) Frisch, M. J.; et al. *Gaussian 03*, revision B.05; Gaussian, Inc.: Pittsburgh, PA, 2003.

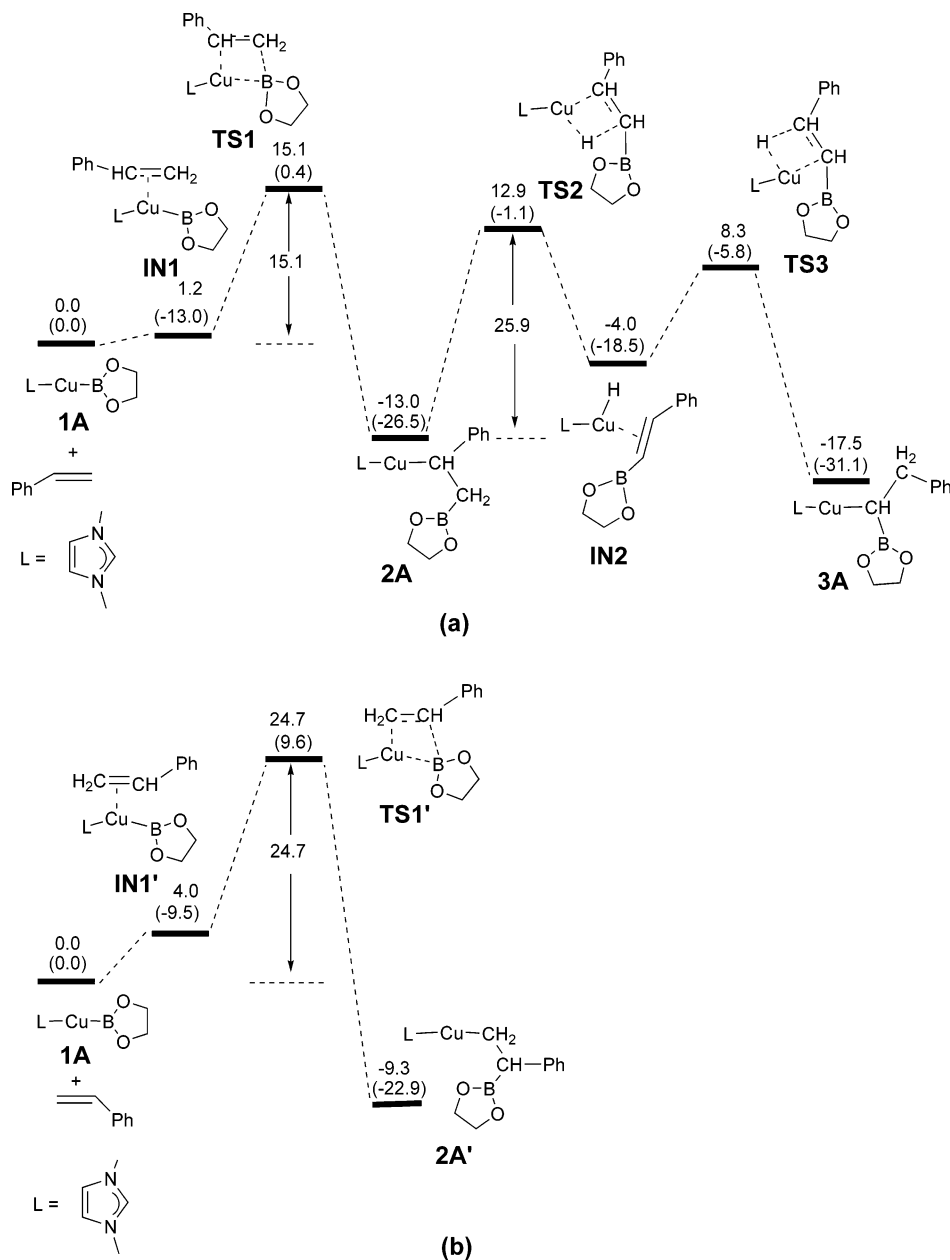


**Figure 1.** (a) Energy profile calculated for the reaction of the model complex (NHC)Cu(boryl) (**1A**) with styrene. (b) Energy profile calculated for 1,2-insertion of styrene into the Cu–B bond in the model complex (NHC)Cu(boryl) (**1A**). The calculated relative free energies and electronic energies (in parentheses) are given in kcal/mol.

insertion of styrene into the Cu–B bond in **1** gives **2**, which then undergoes a rearrangement to generate **3**, an isomer of **2**. In order to investigate the energetics related to the insertion and rearrangement processes, we carried out DFT calculations using the model complex [(NHC)CuB(OR)<sub>2</sub>] {NHC = 1,3-dimethylimidazol-2-ylidene; B(OR)<sub>2</sub> = B(OCH<sub>2</sub>CH<sub>2</sub>O)} (**1A**), in which the substituents at N in the NHC carbene ligand and the methyl groups in the Bpin ligand were replaced by CH<sub>3</sub> and H, respectively. Thus, 1,3-dimethylimidazol-2-ylidene was used to model 1,3-bis(2',6'-diisopropylphenyl)imidazol-2-ylidene (IPr), while B(OCH<sub>2</sub>CH<sub>2</sub>O) was used to model Bpin.

Figure 1a shows the energy profile calculated for the insertion and rearrangement processes. In the figure, the relative free energies (kcal/mol) and relative electronic energies (kcal/mol, in parentheses) are similar in the cases where the number of reactant and product molecules is equal, i.e., in one-to-one or two-to-two transformations, but differ significantly for one-to-two or two-to-one transformations because of entropic contribu-

tions. In this paper, relative free energies are used to analyze the reaction mechanism. For the energy profile shown in Figure 1a, a styrene substrate molecule initially coordinates to the copper center forming a metal- $\eta^2$ -alkene intermediate **IN1**. From **IN1**, the coordinated styrene undergoes a 2,1-insertion into the Cu–B bond via transition state **TS1** to give the  $\beta$ -borylalkyl complex **2A**, a model for the insertion product **2** obtained in the experiment, with a barrier of 13.9 kcal/mol. Then **2A** undergoes a  $\beta$ -hydride elimination to give the copper hydride intermediate **IN2** with a barrier of 25.9 kcal/mol. From **IN2**, a reinsertion occurs to give **3A**, a model for **3**. From the energy profile shown in Figure 1a, we can see that the styrene insertion into the Cu–B bond is relatively more facile than the rearrangement process (**2A**  $\rightarrow$  **IN2**  $\rightarrow$  **3A**). In the rearrangement process, once the  $\beta$ -hydride elimination barrier is overcome, the reinsertion has a barrier of only 12.3 kcal/mol to give the more stable  $\alpha$ -borylalkyl model complex, **3A**. Thus, the theoretical results are consistent with the experimental observa-

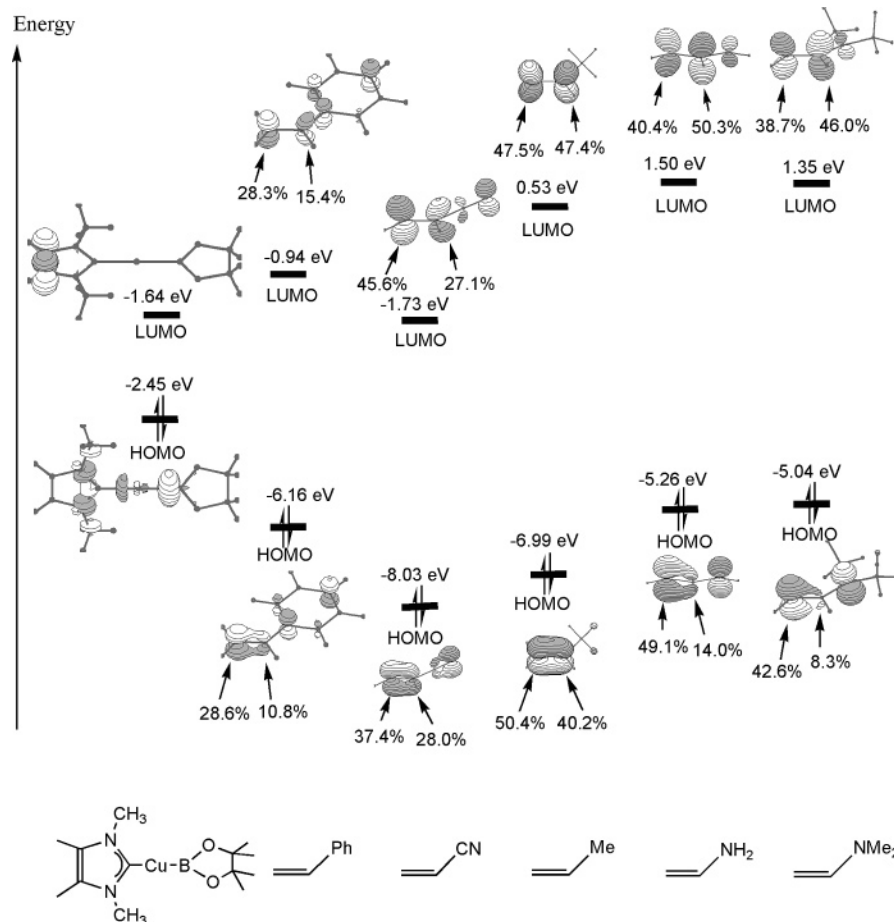


**Figure 2.** Frontier molecular orbitals calculated for the model complex (NHC)Cu(boryl) (**1A**), PhHC=CH<sub>2</sub>, (NC)HC=CH<sub>2</sub>, MeHC=CH<sub>2</sub>, (NH<sub>2</sub>)HC=CH<sub>2</sub>, and (NMe<sub>2</sub>)HC=CH<sub>2</sub>. The orbital energies are given in eV.

tion that **2** is a kinetic product, which can be further transformed to the thermodynamically more stable product **3** after heating.

The products **2** and **3**, in which the Bpin and Ph groups are on different carbons, show clearly the regioselectivity of the styrene insertion; that is, the 2,1-insertion of styrene into the Cu–B bond is preferred over the 1,2-insertion. To compare the two different types of insertion, we also calculated the energy profile for the 1,2-insertion shown in Figure 1b. The results show that the 1,2-insertion is much less favored with a barrier of 24.7 kcal/mol (Figure 1b), consistent with the experimental observation that only the products having the Bpin and Ph groups on different carbons were obtained.

The rearrangement process (**2A** → **IN2** → **3A**) has a barrier of 25.9 kcal/mol (**2A** to **TS2**), which is slightly greater than the barrier of the less favorable 1,2-insertion (24.7 kcal/mol). One reviewer was therefore concerned that the 1,2-insertion may be accessible. However, the 2,1-insertion leading to the formation of **2A** is an irreversible process because the reverse process, from **2A** back to **IN1** or **1A**, has a barrier of 28.1 kcal/mol (Figure 1a), which is greater than the barrier for the rearrangement process from **2A** to **IN2** and then **3**. In other words, the insertion step determines the regioselectivity even though it is not the rate-determining step. As the 2,1-insertion is an irreversible process and is much more favorable when compared with the 1,2-insertion, there is no chance for the 1,2-insertion to occur in the reaction.

**Nature of the Alkene Insertion.** To probe the origins of the regioselectivity, we analyzed the frontier molecular orbitals for both the model complex **1** and the substrate, styrene. Figure 2 shows the spatial plots and orbital energies of the relevant

frontier molecular orbitals. Alkene insertion into a Cu–B bond involves formation of a new B–C bond and a new Cu–C bond and cleavage of the alkene  $\pi$  bond and the Cu–B bond. Therefore, the frontier molecular orbitals that are important in the insertion reaction are the Cu–B  $\sigma$  and  $\sigma^*$  molecular orbitals of **1** and the  $\pi$  and  $\pi^*$  molecular orbitals of the alkene substrate. The Cu–B  $\sigma^*$  molecular orbital lies very high in energy and is not shown in Figure 2, while the Cu–B  $\sigma$  molecular orbital corresponds to the HOMO. Due to the very high lying Cu–B  $\sigma^*$  orbital, better energy matching always exists between the Cu–B  $\sigma$  molecular orbital, the HOMO of **1**, and the alkene  $\pi^*$  molecular orbital, the LUMO of the alkene substrate. Therefore, a key factor that is expected to influence the regioselectivity of the insertion reaction is the interaction between the filled Cu–B  $\sigma$  molecular orbital and the alkene  $\pi^*$  molecular orbital. One can envisage that the direction of electron flow in the insertion reaction is from the Cu–B  $\sigma$  bond to the alkene substrate. In other words, the strong nucleophilicity of the Cu–B bond, which was also emphasized in our studies of the insertion reaction of CO<sub>2</sub> into the Cu–B bond in (NHC)Cu–Bpin complexes,<sup>18</sup> and the electrophilicity of the alkene substrate should both be

(18) (a) Zhao, H.; Lin, Z.; Marder, T. B. *J. Am. Chem. Soc.* **2006**, *128*, 15637. (b) For the relevant experimental work, see: Laitar, D. S.; Müller, P.; Sadighi, J. P. *J. Am. Chem. Soc.* **2005**, *127*, 17196. (c) See also: Laitar, D. S.; Tsui, E. Y.; Sadighi, J. P. *J. Am. Chem. Soc.* **2006**, *128*, 11036. (d) For a recent example of an especially nucleophilic lithium boryl complex, see: Segawa, Y.; Yamashita, M.; Nozaki, K. *Science* **2006**, *314*, 113. (e) See also: Marder, T. B. *Science* **2006**, *314*, 69. (f) For a study of the exceptional *trans*-influence of boryl ligands, related to the electropositive nature of boron and the resulting nucleophilicity of the M–B bond, see: Zhu, J.; Lin, Z.; Marder, T. B. *Inorg. Chem.* **2005**, *44*, 9384.

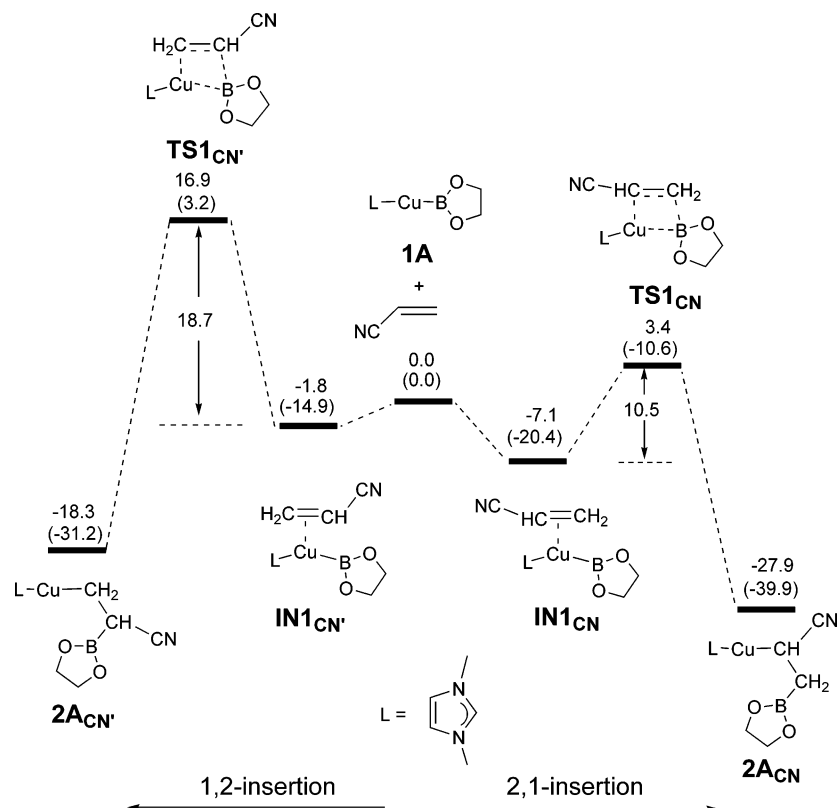


**Figure 3.** Energy profiles calculated for 1,2- and 2,1-insertion of  $\text{CH}_2\text{CHCN}$  with the model complex  $(\text{NHC})\text{Cu}(\text{boryl})$  (**1A**). The calculated relative free energies and electronic energies (in parentheses) are given in kcal/mol.

considered when we try to understand the theoretically calculated reaction barriers and the experimentally observed regioselectivity.

The greater orbital percentage contribution of the  $\text{CH}_2$  carbon versus the phenyl-substituted carbon in the LUMO (Figure 2) of styrene explains the preference for 2,1-insertion over the 1,2-insertion. The  $\pi$ -electron-withdrawing phenyl substituent shifts  $\pi$ -electron density from the  $\text{CH}_2$  carbon toward the phenyl-substituted carbon, making the  $\text{CH}_2$  carbon more electrophilic.

To support the notion that a  $\pi$ -electron-withdrawing substituent favors 2,1-insertion, we also calculated the insertion reaction of acrylonitrile with **1**. Indeed, the 2,1-insertion is much more favored when compared with the 1,2-insertion (Figure 3). The results are also consistent with the relative orbital percentage contribution of the two alkenic carbons in the LUMO of acrylonitrile (Figure 2). The 1,2- and 2,1-insertion barriers of acrylonitrile are respectively much lower than the corresponding insertion barriers of styrene. The lower-lying LUMO of acrylonitrile versus styrene makes the acrylonitrile substrate a better electrophile, reducing both the 1,2- and 2,1-insertion barriers.

To gain further insight into the nature of the alkene insertion, we also studied the insertions of other alkenes having electron-donating substituents such as Me,  $\text{NH}_2$ , and  $\text{NMe}_2$ . The potential energy profiles for the insertion reactions are shown in Figure 4. On the basis of the results we obtained for styrene and acrylonitrile, two distinct observations can be made from Figure 4: (i) the insertion barriers calculated for the three substrates are noticeably higher than those calculated for styrene and acrylonitrile; and (ii) the barriers for the 2,1- and 1,2-insertions of each of the three donor-containing substrates are comparable, whereas styrene and acrylonitrile have significantly different

2,1- and 1,2-insertion barriers; the 2,1-insertion is clearly favored for the acceptor-substituted alkenes.

The first observation can be easily understood. The discussion above shows that the alkene insertion process involves nucleophilic attack of the boryl ligand on the coordinated alkene. Electron-donating substituents make the coordinated alkene more electron-rich and are expected to retard the insertion process. The second observation is quite unexpected. Since electron-withdrawing substituents clearly favor the 2,1-insertion over the 1,2-insertion (Figures 1 and 3), we would therefore expect electron-donating substituents to reverse the preference. The unexpected observation suggests that other factors are also operative in addition to the electronic factor discussed above. Consideration of steric effects can conveniently explain the calculational results. Electronically, electron-donating substituents favor the 1,2-insertion because an electron-donating substituent is able to shift  $\pi$ -electron density toward the  $\text{CH}_2$  carbon, favoring the 1,2-insertion in which the boryl ligand migrates to the  $\text{CH}(\text{X})$  carbon (X: an electron-donating substituent). The transition state for the 1,2-insertion of a given substrate,  $\text{H}_2\text{C}=\text{CH}(\text{X})$ , experiences greater steric repulsion than that of the 2,1-insertion. In both the 1,2- and 2,1-insertion transition states, the C...B distance is much shorter than the Cu...C distance, *vide infra*. Therefore, the repulsive interaction between the substituent X and the pinacolate group on the boryl ligand in the 1,2-insertion transition state is much more significant than that between the substituent X and the NHC ligand in the 2,1-insertion transition state.

The arguments above indicate that for the insertion reaction of  $\text{H}_2\text{C}=\text{CH}(\text{X})$  containing an electron-donating substituent (X) the steric and electronic effects of X have opposite influences on the insertion regiochemistry. For the insertion reaction of

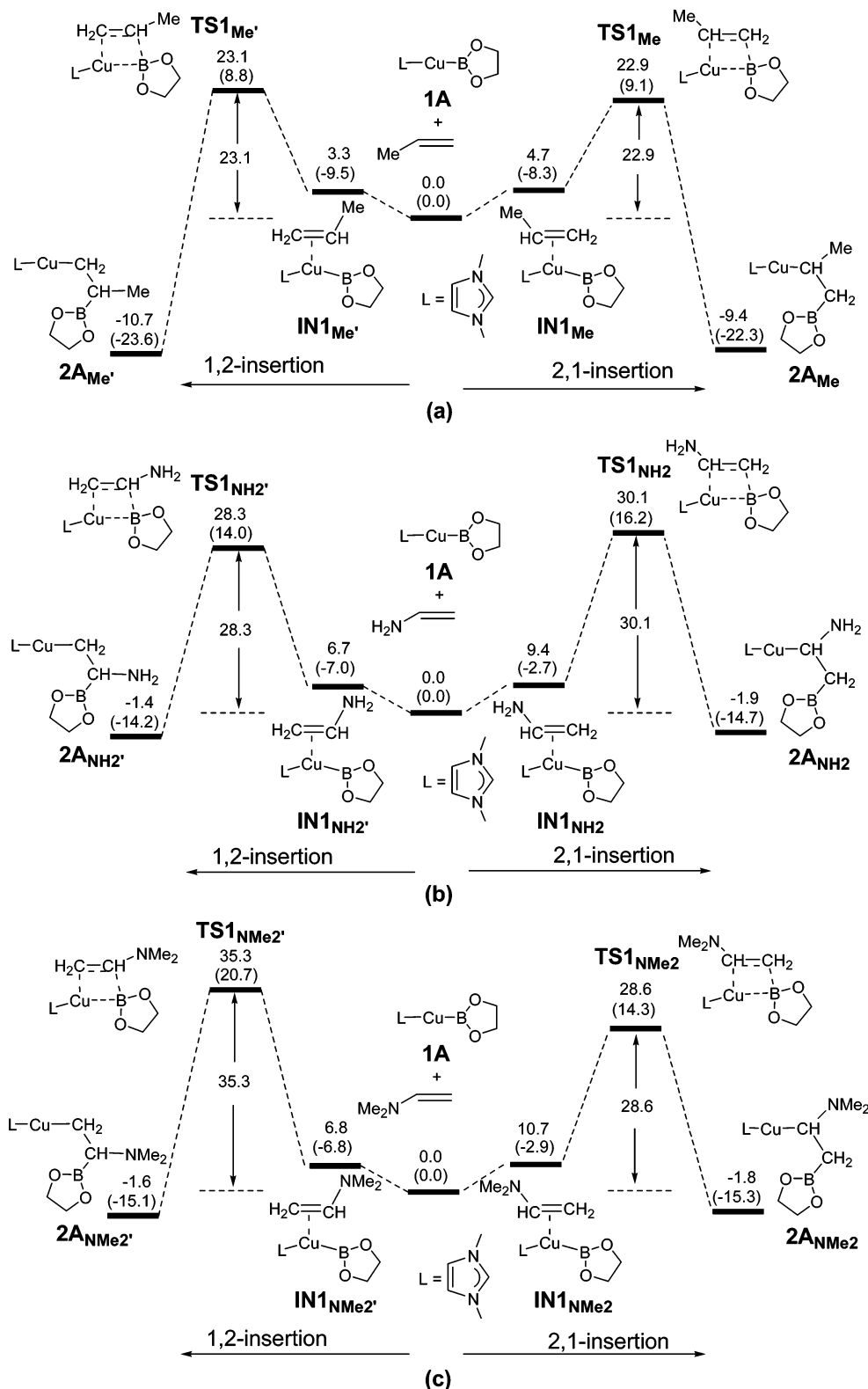


**Figure 4.** Energy profile calculated for 1,2- and 2,1-insertion of  $\text{H}_2\text{C}=\text{CHMe}$  (a),  $\text{H}_2\text{C}=\text{CHNH}_2$  (b), and  $\text{H}_2\text{C}=\text{CHNMe}_2$  (c) into the Cu–B bond in the model complex (NHC)Cu(boryl) (**1A**). The calculated relative free energies and electronic energies (in parentheses) are given in kcal/mol.

$\text{H}_2\text{C}=\text{CH}(\text{X})$  containing an electron-withdrawing substituent (X), both the steric and electronic effects of X favor the 2,1-insertion over the 1,2-insertion, leading to the observation that the 2,1-insertion is clearly favored for styrene as well as acrylonitrile.

The relative barrier heights for the 2,1- and 1,2-insertions shown in Figure 4 reflect how the steric effect counterbalances

the electronic effect for the three substrates containing an electron-donating substituent. For propene, **TS1<sub>Me</sub>** and **TS1<sub>Me'</sub>** have almost the same stability, suggesting that the steric and electronic effects of Me are comparable. For vinylamine, **TS1<sub>NH2</sub>** is slightly higher in energy than **TS1<sub>NH2'</sub>**, suggesting that the electronic effect of  $\text{NH}_2$  is greater than its steric effect. For vinyl-dimethylamine, **TS1<sub>NMe2</sub>** is lower in energy than **TS1<sub>NMe2'</sub>**,

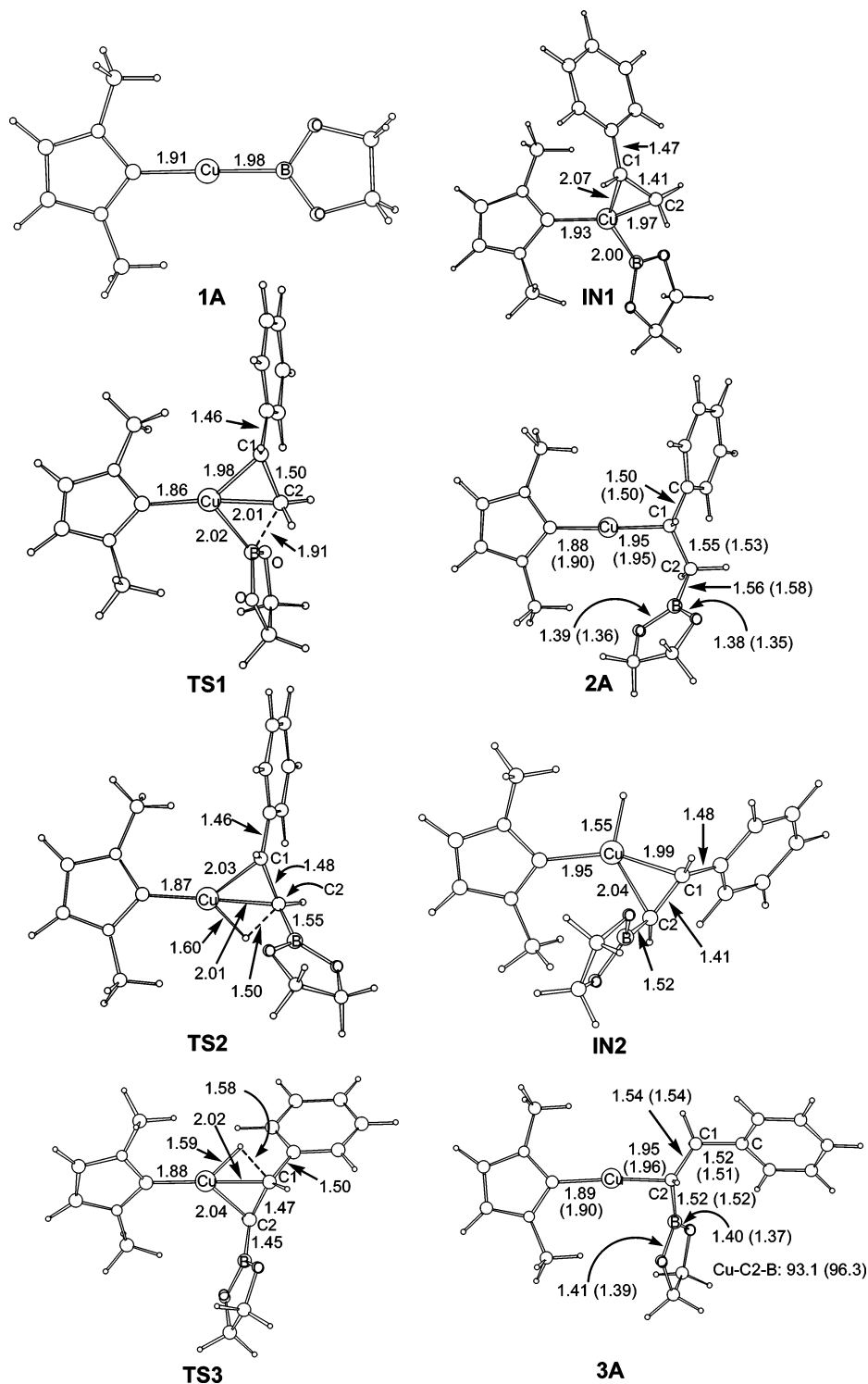


**Figure 5.** Optimized structures with selected structural parameters (distances in Å and angles in deg) for the species shown in Figure 1a. Selected calculated structural parameters for the model complexes 2A and 3A are compared to the experimental structural parameters (in parentheses) of 2 and 3, respectively.

showing that, in this model system, the steric effect of the  $\text{NMe}_2$  group is greater than its electronic effect.

The relative stabilities of the 2,1-insertion and 2,1-insertion products require some comments here. For both the styrene and acrylonitrile substrates, the 1,2-insertion product (2A for styrene or 2A<sub>CN</sub> for acrylonitrile) is noticeably more stable than the 1,2-insertion product (2A' for styrene or 2A'<sub>CN</sub> for acrylonitrile) (see Figures 1 and 3). For the alkyl products, the  $\alpha$  carbon is expected to be electron-rich because it is metal-bonded.

Therefore, electron-withdrawing substituents (Ph or CN) at the  $\alpha$  carbon are expected to exert a stabilizing effect, making the 2,1-insertion product more stable. Steric factors should also favor the 2,1-insertion product because the substituent (Ph or CN) and the boryl group are on different carbons. For each of the three donor-containing substrates (Figure 4), the 1,2- and 2,1-insertion products have similar stabilities, reflecting the balance of both the electronic and steric factors. Electronically, an electron-donating substituent prefers to be

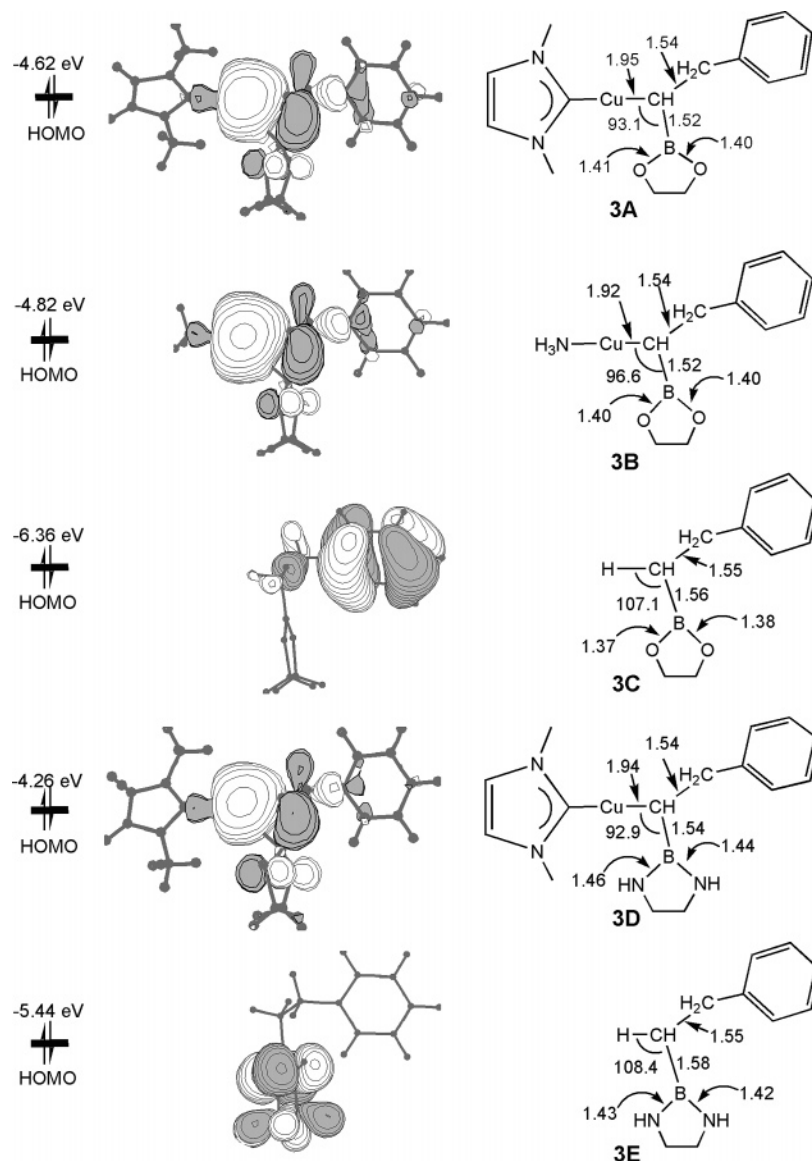


**Figure 6.** Calculated structural parameters (distances in Å and angles in deg) together with spatial plots of the HOMOs calculated for **3A**, **3B**, **3C**, **3D**, and **3E**.

at the  $\beta$  carbon; however, this is sterically unfavorable because both the substituent and the boryl group would be on the same carbon.

Finally, it should be noted that the regioselectivity found here is quite similar to those found in the insertion reactions of alkenes with many neutral Pd(II) complexes.<sup>19</sup> The similarity suggests that in neutral Pd(II) complexes the regioselectivity of insertion of an alkene substrate into a Pd(II)–R (R = H, alkyl, aryl) bond is also related to both the nucleophilicity of the Pd(II)–R bonds and the steric effect of substituents on the alkene. In addition, it is worth noting that in all cases metal-catalyzed dehydrogenative borylation of styrene derivatives gives ArC(R)=CHB(OR')<sub>2</sub> products arising from the regioselective insertion of the alkene into the M–B bond followed by  $\beta$ -hydride elimination.<sup>10</sup>

**Understanding the Small Cu–C–B Angle in the  $\alpha$ -Borylalkyl Complex **3**.** As mentioned in the Introduction, the structure of the  $\alpha$ -borylalkyl complex, **3**, determined by single-

crystal X-ray diffraction, shows that the Cu–C–B angle is unexpectedly small (96.3(2)°).<sup>7d</sup> The calculated Cu–C–B angle in the model complex **3A** is also small (93.1°) (Figure 5). The long Cu–B distance (2.608(3) Å) and the trigonal geometry about boron in the crystal structure do not suggest an attractive Cu–B bonding interaction. The solution <sup>11</sup>B NMR spectrum of the complex does not give any indication of such an attractive interaction.<sup>7d</sup>

We first examined the HOMO calculated for the model complex **3A** (Figure 6), which corresponds mainly to a filled Cu–C ( $\alpha$ -borylalkyl)  $\sigma$ -bonding orbital. The bonding characteristics of the HOMO show that there also exists a slight mixing of 2p <sub>$\pi$</sub>  orbitals from the two oxygen atoms as well as the boron atom of the boryl group. The 2p <sub>$\pi$</sub>  orbitals from the two oxygen atoms and the boron atom interact in a  $\pi^*$ -antibonding fashion. The slight mixing of the  $\pi^*$  orbital from the boryl group into the HOMO suggests a charge transfer from the filled Cu–C ( $\alpha$ -borylalkyl)  $\sigma$  bond to the “empty” p<sub>z</sub> orbital on boron (i.e., the  $\pi^*$  orbital from the boryl group). The charge transfer stabilizes the high-lying HOMO, which corresponds to the Cu–C ( $\alpha$ -borylalkyl)  $\sigma$ -bonding orbital. Clearly, a small Cu–C–B angle, which enhances the orbital mixing,

(19) (a) Michalak, A.; Ziegler, T. *Organometallics* **1999**, *18*, 3998. (b) Michalak, A.; Ziegler, T. *Organometallics* **2000**, *19*, 1850. (c) Deeth, R. J.; Smith, A.; Brown, J. *J. Am. Chem. Soc.* **2004**, *126*, 7144. (d) Cabri, W.; Candiani, I. *Acc. Chem. Res.* **1995**, *28*, 2.



maximizes the stabilizing effect. In essence, this reflects a small degree of C–B  $\pi$  bonding (i.e., hyperconjugation) or, more accurately, (Cu–C)–B  $\pi$  bonding, as the Cu–C  $\sigma$ -bonding orbital is a much better  $\pi$ -donor than the lower lying oxygen p orbitals.

To support the charge transfer (hyperconjugation) argument above, we rotated the boronate plane in **3A** by 90° and performed a partial geometry optimization by freezing the relevant dihedral angle. The partially optimized structure is ca. 10 kcal/mol higher in energy than the fully optimized structure **3A**. In the partially optimized structure, the Cu–C–B angle is 106.8°, which is not unusual, indicating that the hyperconjugation interaction is absent in the partially optimized structure.

To add further support to the charge transfer argument above, we examined the model complex **3B**, in which the NHC ligand is replaced with NH<sub>3</sub>. We expect a smaller charge transfer because the Cu–C ( $\alpha$ -borylalkyl)  $\sigma$ -bonding orbital is stabilized due to the fact that NH<sub>3</sub> exerts a weaker trans influence than NHC. Indeed, the Cu–C–B angle calculated for **3B** is larger than that calculated for **3A**, 96.6° versus 93.1° (Figure 6). The HOMO calculated for **3B** lies lower in energy than that calculated for **3A**, –4.82 eV vs –4.62 eV. The Cu–C ( $\alpha$ -borylalkyl)  $\sigma$  bond calculated for **3B** is shorter than that calculated for **3A**, 1.92 Å versus 1.95 Å. When the metal fragment is replaced with a hydrogen atom (see **3C** in Figure 6), the calculated H–C–B angle in **3C** approaches the expected tetrahedral angle because the HOMO is a  $\pi^*$  orbital of the phenyl group instead. The B–C bond in **3C** is longer than those in **3A** and **3B** because the charge transfer interaction, which increases the C–B ( $\pi$ ) bonding, no longer exists.

We also examined the model complex **3D** (Figure 6) in order to see whether the lone pairs on the two nitrogen atoms of the boryl group could turn off the function of the “empty” orbital on the boron center and reduce the charge transfer because B–N  $\pi$ -bonding interactions are expected to be much stronger than B–O  $\pi$ -bonding interactions. To our surprise, the Cu–C–B angle calculated for **3D** (92.9°) is almost the same as that calculated for **3A** (93.1°) (Figure 6), suggesting that the (Cu–C)–B  $\pi$ -interaction still dominates the bonding. Compared to **3E**, in which the (NHC)Cu is replaced by H and thus the charge transfer is not possible, model complex **3D** has longer B–N bonds, supporting the suggestion that the B–N  $\pi$ -bonding interactions in **3D** are not that significant. Similarly, the B–O bond distances in **3A**, **B** are also noticeably longer than those in **3C**. Comparing the structural parameters for **3A** (or **3**) with those for **2A** (or **2**), the B–O bond distances in **3A** (or **3**) are also systematically longer than those in **2A** (or **2**) (Figure 5). In **3A** (or **3**), the charge transfer is possible. In **2A** (or **2**), the charge transfer is not possible because the Cu–C  $\sigma$  bond, which corresponds to a high-lying occupied orbital, and the boryl group are separated by a C–C  $\sigma$  bond (Figure 5).

The hyperconjugation interaction discussed above explains well the small Cu–C–B angle observed in **3**. Interestingly, the Cu–C(alkyl) bond in **3** (or **3A**) does not show an appreciable lengthening because of the hyperconjugation interaction when compared with the Cu–C(alkyl) bond in **2** (or **2A**) (Figure 5). An explanation for this is that there is Cu–C(alkyl) bond hyperconjugation in **2A** as well with the C1-bonded phenyl  $\pi^*$  orbitals. The C1–C(phenyl) bond distance in **2** or **2A** is found to be shorter than that in **3** or **3A**.

## Conclusions

The insertion reactions of alkenes into Cu–B bonds in copper(I) boryl complexes have been investigated by DFT calculations. The computational results support the notion that insertion of an alkene substrate molecule into a Cu–B bond involves nucleophilic attack of the boryl ligand on the coordinated alkene. Therefore, alkenes bearing an electron-withdrawing substituent have smaller insertion barriers than those bearing an electron-donating substituent. The nucleophilicity of boryl ligands (the electron-richness of metal–boryl bonds) also influences the regiochemistry of the insertion reactions. For alkenes bearing an electron-withdrawing substituent, 2,1-insertion, i.e., migration of the boryl ligand to the unsubstituted carbon, is preferred over 1,2-insertion. However, the factors governing the insertion regioselectivity are more complicated for alkenes bearing an electron-donating substituent, as electronic and steric effects of an electron-donating substituent have opposing influence, and 2,1- and 1,2-insertions have comparable transition state energies.

Similar to a Cu–B(boryl) bond, a Cu–C(alkyl) bond is also very electron-rich. When there is a boryl substituent at the metal-bonded carbon, the electron-rich Cu–C bond can interact with the “empty” p orbital on boron, resulting in  $\pi$  bonding between the filled Cu–C ( $\alpha$ -borylalkyl)  $\sigma$  bond and the  $\pi^*$  orbital of the boryl group (the “empty” p orbital on boron). We expect that similar bonding scenarios (hyperconjugation) should also exist in other metal complexes containing an M–C–B linkage, leading to small M–C–B angles.

**Acknowledgment.** This work was supported by the Research Grant Council of Hong Kong (HKUST 6023/04P and DAG05/06.SC19). T.B.M. thanks the Royal Society (UK) for support via an International Outgoing Short Visit Grant. The authors thank Professor Pedro Pérez for a preprint of ref 8p.

**Supporting Information Available:** Complete ref 17 and tables giving Cartesian coordinates and electronic energies for all of the calculated structures. This material is available free of charge via the Internet at <http://pubs.acs.org>

OM070103R